IL NUOVO CIMENTO Vol. 34 C, N. 5 Settembre-Ottobre 2011
DOI 10.1393/ncc/i2011-10960-4

Communications: SIF Congress 2010

Simultaneous morphological and functional imaging of the honeybee's brain by two-photon microscopy

A. Haase(*)

Dipartimento di Fisica e Centro di Ricerca BIOtech, Università di Trento via delle Regole 101, Mattarello, 38100 Trento, Italy

(ricevuto l' 11 Gennaio 2011; approvato il 2 Marzo 2011; pubblicato online il 19 Settembre 2011)

Summary. — Thanks to its rather simply structured but highly performing brain, the honeybee (*Apis mellifera*) is an important model for neurobiological studies. Therefore there is a great need for new functional imaging modalities adapted to this species. Herein we give a detailed report on the development and performance of a platform for *in vivo* functional and morphological imaging of the honeybee's brain, focusing on its primary olfactory centres, the antennal lobes (ALs). The experimental setup consists of a two-photon microscope combined with a synchronized odour stimulus generator. Our imaging platform allows to simultaneously obtain both morphological measurements of the ALs functional units, the glomeruli, and *in vivo* calcium recording of their neural activity. We were able to record the characteristic glomerular response maps to odour stimuli applied to the bee's antennae. Our approach offers several advantages over the commonly used conventional fluorescence microscopy. Two-photon microscopy provides substantial enhancement in both spatial and temporal resolutions, while minimizing photo damage. Calcium recordings show a more than fourfold improvement in the functional signal with respect to the techniques available up to now. Finally, the extended penetration depth, thanks to the infrared excitation, allows the functional imaging of profound glomeruli which have not been optically accessible up to now.

PACS 87.19.lt – Sensory systems: visual, auditory, tactile, taste, and olfaction.
PACS 87.19.lh – Optical imaging of neuronal activity.
PACS 87.64.mn – Multiphoton.

1. – Introduction

Many of the important advances in neuroscience have been linked to the development of new investigative tools. The action potentials of single neurons have been measured for

(*) E-mail: albrecht.haase@unitn.it

the first time by intracellular recording [1]. A next important step was the development of a new class of voltage-sensitive dyes [2], which offered the possibility of optically imaging the functionality of neuronal circuits at the level of single neurons as well as the whole brain. In recent years, the development of calcium-sensitive dyes [3] had an incredible impact on functional neuroimaging, providing a universal and sensitive method to study distinct information processing pathways in whole neural networks. A further improvement was brought by two-photon laser scanning microscopy [4], which via calcium recording allowed for *in vivo* real-time monitoring of complex neural circuits down to several hundred micrometers within the specimen [5].

This communication reports our experimental efforts in two-photon calcium imaging of the honeybee brain. With less than one million neurons, the honeybee is an excellent model for the study of neural systems of intermediate complexity [6], and its brain's dimensions of approximately $2.5\,\mathrm{mm} \times 1.6\,\mathrm{mm} \times 0.8\,\mathrm{mm}$ [7] make it an ideal candidate for two-photon microscopy [8]. In the past years, several different optical-imaging approaches have allowed to gain tremendous insights into the bee's olfactory system. Along the antennae $\sim$ 60000 olfactory receptor neurons (ORNs) send their axons to the primary processing centres in the brain, the antennal lobes (ALs). These consist of 160 functional units, synaptic centres called glomeruli, each of them connected to one odour receptor family only. The glomeruli interact via $\sim$ 4000 local interneurons. The ALs can be subdivided into 4 regions named T1–T4 [9], with a fundamental difference in how they relay via the $\sim$ 950 projection neurons (PNs) to the higher brain centres. Class T1 projects along the lateral antenno-cerebralis tract (l-ACT) first into the lateral horn (LH) and then into the mushroom body (MB), while the other classes T2–T4 project along the median antenno-cerebralis tract (m-ACT) first into the MB and then into the LH [10].

Early pioneering works in functional imaging of this system using voltage-sensitive dyes [11] have paved the way for a series of extremely successful experiments using optical-fluorescence microscopy and various staining techniques to investigate different aspects of the odour processing network. A first breakthrough in the systematic description of the odour coding in the AL was achieved by using calcium-sensitive cell-permeant dyes which allowed visualizing the activity patterns of a big part of the T1 glomeruli [12]. These signals were found to be dominated by the ORNs, the input channels to the AL. The method of selective backfill staining of specific neurons with membrane-impermeable dyes [13] has instead allowed to record the AL's output signal from the PNs [14].

Besides the functional imaging studies also the morphology of the olfactory centres has been investigated extensively [9], more recently by confocal microscopy [15, 7], and evidence of strong glomerular plasticity in the ALs has been reported lately [16]. While linear microscopy techniques have been proven over the last years to be very effective in characterizing basic principles of this complex neuronal system, their intrinsic limitations have become more and more obvious [17]. Wide-field microscopy does not offer sufficient axial resolution to pinpoint the exact origin of functional signals from deeper glomeruli and lacks the temporal resolution to determine whether valuable information might be encoded in the temporal structure of the recorded odour-evoked signals. Whereas confocal microscopy due to its intrinsic photo-damaging properties poses severe time constraints to *in vivo* imaging sessions and has therefore only been used for morphological studies of the dissected and embedded brain.

In this paper we give a detailed report on our neural imaging platform for functional imaging of the honeybee's antennal lobe [18]. Our system permits to overcome the imaging impediments currently faced by neuroscientists. It enables us to acquire both *in vivo* functional and morphological data from the ALs. Functional data show that

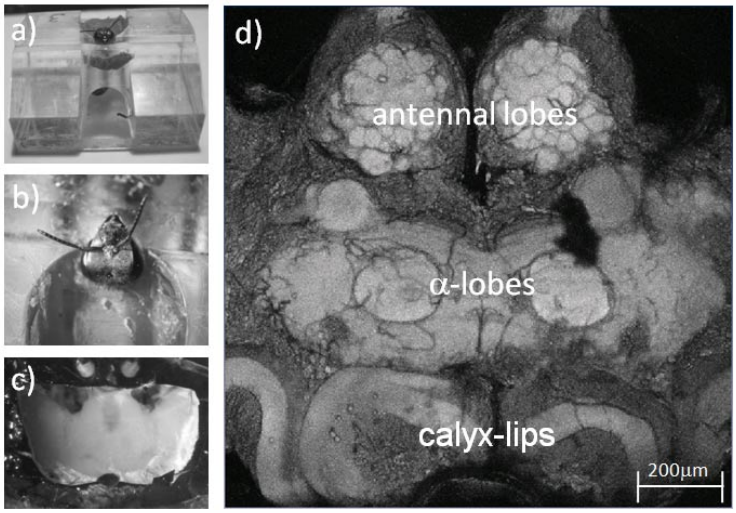

Fig. 1. – a), b) Bee attached to the imaging stage. c) Exposed brain, after the cuticula has been opened and glands and trachea have been removed. d) Morphological image of a big part of the honeybee brain, acquired with a 10× lens with a field of view of 1.2 mm, after bath staining with the membrane-selective dye RH795 (Invitrogen). It allows the identification of the antennal lobes and the mushroom body with its α-lobes and calyx lips. These images help finding the correct injection position into the antenno-cerebralis tracts for antennal lobe backfill staining.

we have been able, for the first time, to longitudinally resolve active glomeruli, while the high temporal resolution permits a reconstruction of the neuron's firing rate [19]. Besides the well-investigated T1 glomeruli, projecting into the l-ACT, the intrinsic two-photon optical penetration is deep enough to study also the other glomeruli classes T2 and T3 projecting into the m-ACT, which have not been optically accessible in the ALs yet. Electrophysiological studies [20, 21] and imaging of their axon terminals [22] have suggested distinctive functional differences with respect to the l-ACT glomeruli.

2. – Methods

Bees have been collected from outdoor hives and prepared in accordance to a well-established protocol [23]. After chilling to immobility, bees were fixed to a custom-made imaging stage (fig. 1(a,b)) using dental waxes (Kerr; Siladent). A window was cut into the head's cuticula above the antennal lobes and mushroom body, glands and trachea were gently moved aside (fig. 1(c)), and a solution of calcium-sensitive dye (fura2-dextran, Invitrogen) and 2% Bovine Serum Albumin (Sigma-Aldrich) was injected by dye-coated micro-tips into the antenno-cerebralis tracts below the α-lobe (fig. 1(d)). Finally, the cuticula was carefully closed and the animals were stored for 20 h in a dark, cool, and humid place in order for the dye to diffuse into the AL. Before the imaging session, the cuticula, the glands, and the trachea above the AL were removed. A pond was formed above the imaging region using plastic plates, sealed with silicon (Kwik-Sil, WPI), and filled with specific Ringer's solution [23], imitating the brain's natural environment. The imaging setup is sketched in fig. 2. It consists of a two-photon microscope (Ultima IV, Prairie Technologies) combined with an ultra-short pulsed laser (Mai Tai Deep See HP,

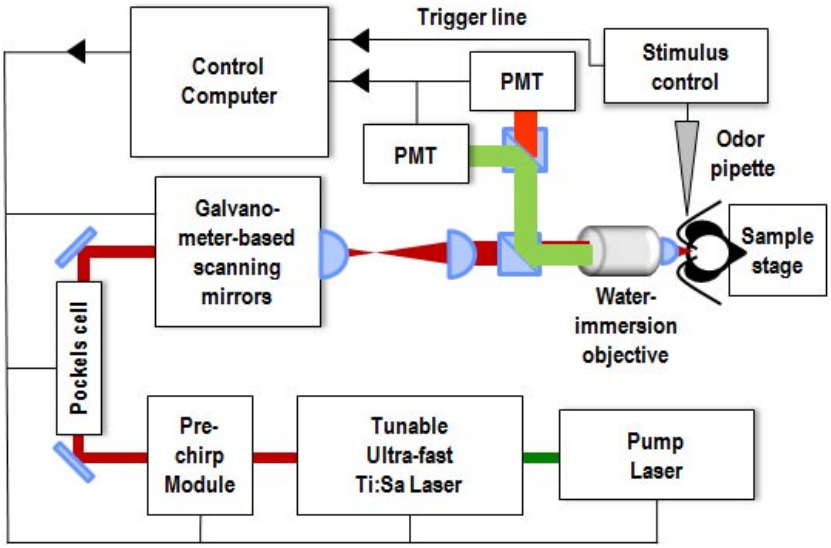

Fig. 2. – a) Experimental setup: A tunable ultra-fast pulsed laser serves as the light source. After pulse shaping in a pre-chirp module and intensity control by a Pockels cell, the beam is scanned by galvo-mirrors and focused by a water immersion objective to the exposed AL of a bee, fixed to a mounting stage. The fluorescence signal is collected in reflection, separated by way of a dichroic mirror and detected by photomultiplier tubes (PMT). A stimulus controller produces time-gated odour puffs which are synchronized with all command signals and acquisitions by a common gate.

Spectra-Physics). The laser was tuned to 800 nm for resonant excitation of the free fluorophore fura-2. The two-photon absorption is optimized by pulse re-shaping for dispersion compensation in a pre-chirp module. A Pockels cell controls the beam intensity and galvo-mirrors allow fast and variable scanning. The beam is strongly focussed onto the sample by a water-immersion objective (40×, NA 0.8, Olympus). Fluorescence is collected in reflection by the same objective, separated from the backscattered excitation light by a dichroic beam splitter, filtered by a 70 nm band-pass filter centred at around 525 nm (both Chroma Technology), and detected by Photomultiplier tubes (Hamamatsu Photonics). A point-spread function measurement verified the microscope's resolution to be diffraction limited to $\sigma_{x,y} = 230\,\text{nm}$ in the plane and $\sigma_z = 1.1\,\mu\text{m}$ axially. Optimal signal-to-noise ratio was achieved with laser powers of about 10 mW at the sample surface without observing any induced photo damage during the measurement. The temperature of the experimental environment was stabilized to 29 °C.

To allow for recordings with temporal resolution as high as 15 ms, the excitation laser was scanned in an arbitrary horizontal plane along one-dimensional custom-defined traces (fig. 3(a)). These line scan traces were chosen to cross all glomeruli of interest (fig. 3(b)). All acquired data have been corrected for photobleaching, while 2D running-average filtering was used to reduce the noise level. Spatial averaging was performed over a typical glomerulus size of 30 μm, while temporal averaging was applied over 80 ms preserving all main dynamic features of the data.

A stimulus controller (CS-55, Syntech) delivered odour stimuli to the bee's antennae without changing the total air flux to avoid mechanical stimuli. The odour puffs come from Pasteur pipettes in which 10 μL of an odour solution (1:10 in mineral oil) were deposited on a piece of filter paper.

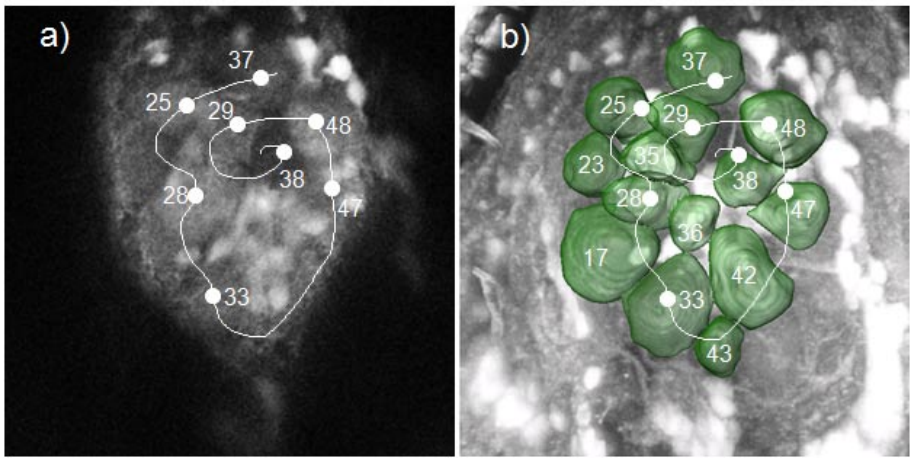

Fig. 3. – a) Image of a left antennal lobe at 25 μm depth: The line indicates the laser scanning trace, the dots label the measurement's reference positions corresponding to the vertical lines in fig. 4. (b) Axial projection view of the AL volume image stack, superimposed by the reconstructed surface plots of the T1 glomeruli crossed by the scanning trace. The glomeruli are identified and labelled according to [15].

All command signals and acquisitions were controlled by a common gate which allows precise synchronization of the involved pulses. The experimental cycle began by starting the image acquisition. After 3 s the stimulus generator received a trigger releasing an odour puff of 2 s length. The exact arrival time of the odour at the bee antenna was measured and found to be stable within 10 ms, which allows for accurate measurements of the neuronal response delay. After 9 s image acquisition stopped and automatic data evaluation started.

Response recordings were repeated three times with the same stimulus with one minute recovery intervals in between. Averaging over these data sets is applied if only the total response strength is of interest. This serves to reduce random fluctuations and becomes especially useful at greater imaging depths.

Thanks to the reduced photo-damage characteristics of two-photon microscopy, due to the limited absorption volume in the sample, the imaging sessions could be extended up to 5 hours before we noticed an essential drop in the brain activity.

Data analysis was automatically executed during the experiments by Matlab (Mathworks) scripts. Later post-processing for 3D reconstruction, image segmentation, and volumetric measurements was performed using the software Amira (Visage Imaging).

3. – Results

In a first experiment, we recorded the spatio-temporal functional activity in the AL by measuring the two-photon calcium response signal along the line traces indicated in fig. 3. To compare the performance of our imaging setup with conventional methods, we used as odour stimuli three well-studied floral components [24]: 1-Nonanol, 1-Octanol, and 1-Hexanol. Enhanced neural activity leads to an increasing intra-neuronal calcium concentration, the fluorophore binds more calcium and its absorbtion spectrum is shifted away from the laser excitation wavelength. This causes a drop in the measured two-

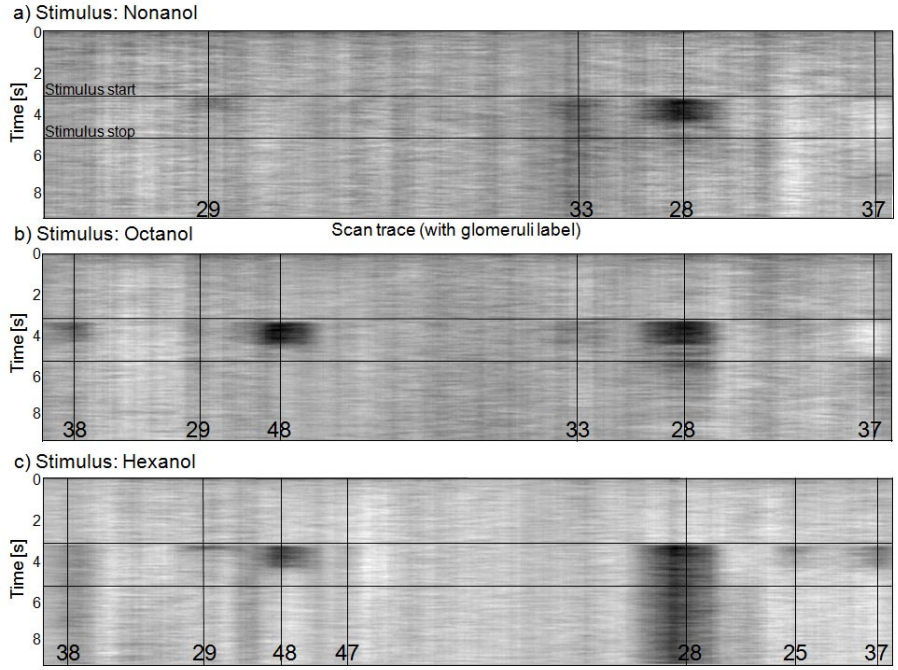

Fig. 4. – Calcium response maps for three different odour stimuli: (a) 1-Nonanol, (b) 1-Octanol, and (c) 1-Hexanol. Temporal changes along the scanning trace in fig. 3 are mapped. The x-axis shows the scan line, the y-axis time, the stimulus period after 3 s is enclosed by the horizontal lines, the responding glomeruli centres are marked by vertical lines, the numbers label the identified T1 glomeruli according to [15].

photon fluorescence intensity, manifesting in dark bands in the scanlines-over-time maps at the positions of the corresponding glomeruli. We detected response signals of more than 20% intensity change, which is more than 4 times higher than in comparable experiments using wide-field imaging. The recorded odour response maps are shown in fig. 4 and reproduce features which have already been observed by conventional single-photon fluorescence microscopy, such as the very strong response of glomerulus T1-28 to all tested odours. Its response strength increases with a decreasing odour's carbon chain length, while the weaker response of T1-33 increases with the carbon chain length [25,24]. Likewise, it has been found that 1-Hexanol produces the broadest response spectrum of the tested odours. Strikingly different from the previously published data obtained with wide-field microscopy [24] are the quite strong responses of glomeruli T1-48 to 1-Octanol and 1-Hexanol and the strong inhibitive response of T1-37 to 1-Nonanol and 1-Octanol, which might be due to the enhanced sensitivity of our imaging system.

The high temporal resolution is demonstrated in fig. 5 where the single response curves to all tested odours of the strongest responding glomerulus T1-28 are depicted. The time resolution and the precise stimulus synchronization allow a systematic investigation of response delays and their dependence on the odour stimuli, as well as the specificity of the observed oscillatory features. Both response latency [20] and synchronized oscillations [26], previously observed in electrophysiological measurements, are hypothesized to be part of a general odour code.

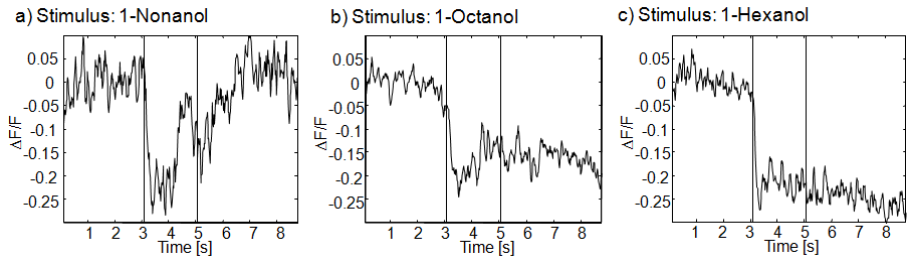

Fig. 5. – Single temporal-response functions of the strongest responding glomerulus T1-33 in the maps in fig. 4, stimulated by 1-Nonanol in (a), 1-Octanol in (b), and 1-Hexanol in (c). The relative change in fluorescence is plotted as a function of time, the stimulus period after 3 s is enclosed by vertical lines.

Finally, we have exploited the larger penetration depth and the higher axial resolution offered by our setup. In fig. 6(a) we present a morphological image stack down to 270 μm, where the most profound glomeruli are located. We restrict the volumetric reconstruction of the single glomeruli to a depth of $\approx$ 200 μm, down to which we were so far able to identify glomeruli with certainty. Figure 6(b) shows a projection view along the anterior-posterior axis (above) together with a surface plot of the identified glomeruli (below). Figure 6(c) shows a projection view along the dorso-ventral axis together with the identified glomeruli. Figure 6(c) shows the depth limit for obtaining morphological information is $\approx$ 400 μm. The reconstructed glomeruli have the following color code: the green ones belong to the T1 sensory group projecting into the l-ACT axonal tract, while the blue and red coloured ones belong to the deeper laying T2 and T3 groups, respectively,

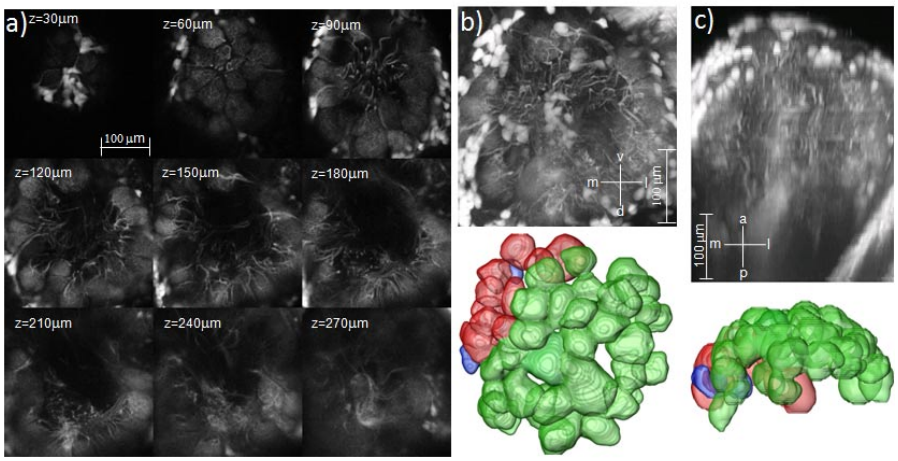

Fig. 6. – (Colour on-line) a) Image stack examples down to 270 μm penetration depth into the right AL. b) Projection view along the anterior-posterior axis (above) and reconstructed glomerular volume images (below). c) Projection view along the dorso-ventral axis (above) and reconstructed glomerular volume images (below). Glomeruli coloured in green are from the T1 region projecting into the l-ACT, the blue glomeruli are from the T2 region, the red ones from the T3 region, the last two projecting into the m-ACT.

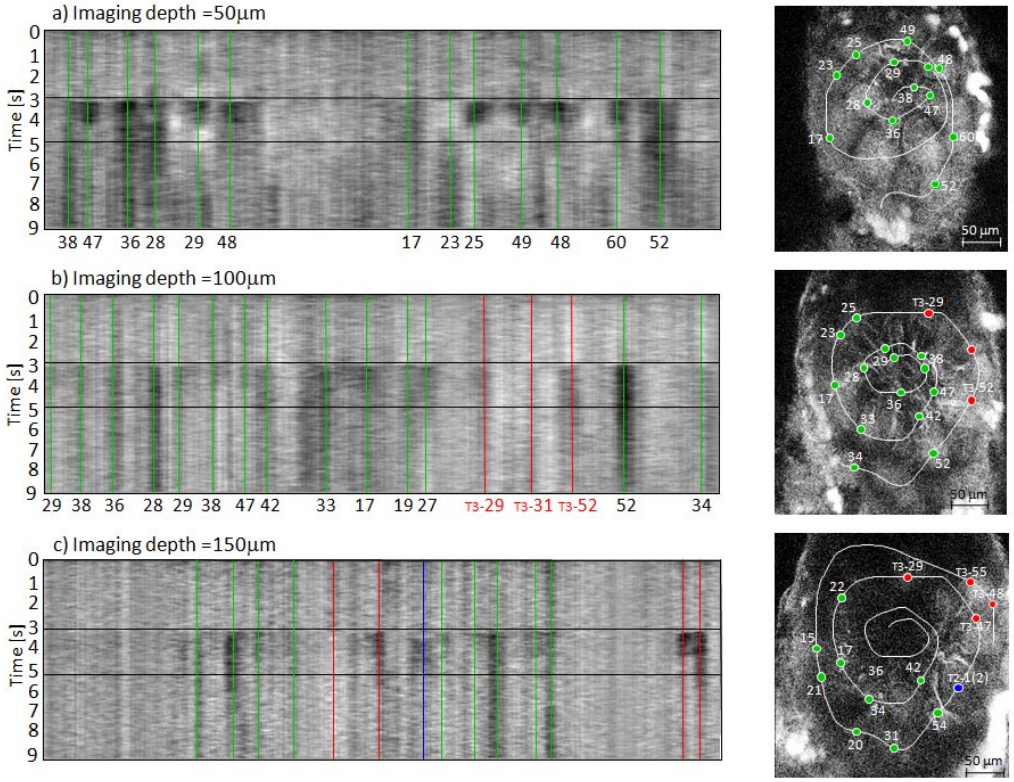

Fig. 7. – Odor response maps of a left AL to 1-Hexanol stimuli recorded at different imaging depth: 50 μm in (a), 100 μm in (b), and 150 μm in (c). The calcium response maps are shown together with the imaging planes and the corresponding laser scan traces. The responding centres are labelled by the corresponding glomerular number. T1 glomeruli are labelled by numbers only, the others by the sensor tract T2, T3, respectively, and the corresponding number.

both projecting into the m-ACT. Apart from a few exceptions, the T2 and T3 glomeruli have never been optically accessible *in vivo* because of their position below the surface or below the penetration depth limit of conventional microscopy.

The maximum penetration depth for clear functional imaging was found to be 150 μm. Figure 7 shows odour response maps to a 1-Hexanol stimulus at different depths within the AL. The high axial resolution shows strongly changing response pattern at the different depths, due to the contribution of different glomeruli. The identified glomeruli are marked and labelled according to [15]. The green coloured points represent signals from the T1 tract. In some of the cases the glomeruli are located in an upper layer above the imaging plane and the signal comes only from the few projection neurons connected to them. In these cases, the absolute fluorescence signal is very faint, but, nevertheless, a relative drop of up to 20% can be detected also here. The data points coloured in blue and red mark glomeruli from the T2 and T3 tract, respectively. These glomeruli are located in the focal plane leading to a strong absolute fluorescence signal. For the first time we were able to optically record activity also from these glomeruli deep within the antennal lobe.

The response of the surface glomeruli was compared to experiments using wide-field fluorescence [12, 24]. In most of the cases the normalized response signals agree to the reported values or are found to be slightly higher, which might be explained by the higher sensitivity of our imaging system. The main responses to 1-Hexanol are coming from glomeruli T1-28, T1-36, and T1-52. Among the T1-glomeruli imaged for the first time, the most strongly responding glomeruli are T1-20 and T1-34. Glomerulus T1-23 shows a strong inhibitive response. The T3 glomeruli, most of them imaged for the first time, show mainly responses of medium strength and duration. The first image of a glomerulus of the T2 class (T2-1(2)) shows as a characteristic an extremely long response delay, which confirms electrophysiological studies [20, 21].

These data demonstrate that we created optical access to the profound glomeruli of the T2 and T3 classes projecting into the m-ACT and thus made straight path to the exploration of a whole new branch of the olfactory processing network, which so far could be investigated only partially by electrophysiological methods [20, 21] or at the level of the axon terminals [22]. Strong activity signals and high temporal resolution are also here giving hope to a much needed systematical expansion of the odour response maps by including these new glomerular classes.

4. – Conclusion

The functional data acquired by the two-photon microscopy we have presented in this work show that our imaging platform offers the possibility to extend the specific AL odour response maps which have been measured in the past for many different odour components and in most of the T1 glomeruli [12]. So far these maps contain only the static parameters response strength and consistency range. This might now be completed by temporal features as the response latency or oscillatory components, if further experimental studies prove a specificity of these features. The intrinsic axial resolution and the extended imaging depth of two-photon microscopy has for the first time allowed to record profound functional data. Odor response maps could therefore be further completed by data from the glomerular classes T2, T3, and T4.

This new access to sub-surface glomeruli is of special interest because these glomerular classes are projecting into the m-ACT axonal tract and have been hypothesized to show fundamental differences regarding their odour coding properties [20-22], as well as their memory-related plasticity after odour conditioning [24]. The morphological division of the olfactory pathway into the two axonal tracts [10] seems to be accompanied by a functional division into two parallel processing branches. We have now, for the first time, created optical access to the m-ACT branch in the antennal lobe which allows a systematic study of the complete odour code.

Moreover, the intrinsically high spatial resolution causes a more than 4-fold increase in the functional-related fluorescence change with respect to similar experiments using wide-field imaging. Another promising feature of the two-photon microscopy approach is the possibility to investigate sub-glomerular structures down to single neurons [8]. This becomes even more crucial if the imaging is extended to higher-order brain centres such as the mushroom body, where a meta-structure comparable to the ALs glomeruli is absent [27].

Finally, aside from the resolution's improvements, the intrinsic two-photon limited photo-damage has allowed extended imaging sessions up to 5 hours. This offers the exciting possibility of future *in vivo* real-time studies of the antennal lobe plasticity after odour conditioning [16].

* * *

I gratefully acknowledge the support of my co-workers involved in this project: E. Rigosi (CIMeC, University of Trento and IASMA, Fond. E. Mach, S. Michele), F. Trona (IASMA), G. Anfora (IASMA), G. Vallortigara (CIMeC), C. Vinegoni (CSB, MGH, Harvard Medical School), and R. Antolini (Physics Dept., University of Trento). The project was funded by the Provincia Autonoma di Trento (project COMNFI).

REFERENCES

[1] Hodgkin A. L. and Huxley A. F., *Nature*, **144** (1939) 710.
[2] Salzberg B. M., Cohen L. B. and Davila H. V., *Nature*, **246** (1973) 508.
[3] Grynkiewicz G., Poenie M. and Tsien R. Y., *J. Biol. Chem.*, **260** (1985) 3440.
[4] Denk W., Strickler J. and Webb W., *Science*, **248** (1990) 73.
[5] Svoboda K., Denk W., Kleinfeld D. and Tank D. W., *Nature*, **385** (1997) 161.
[6] Menzel R. and Giurfa M., *Trends Cogn. Sci.*, **5** (2001) 62.
[7] Brandt R., Rohlfing T., Rybak J., Krofczik S., Maye A., Westerhoff M., Hege H.-C. and Menzel R., *J. Comp. Neurol.*, **492** (2005) 1.
[8] Franke T., *In vivo 2-photon calcium imaging of olfactory interneurons in the honeybee antennal lobe*, Dissertation (FB Biologie, Chemie, Pharmazie, Freie Universität Berlin) 2009.
[9] Flanagan D. and Mercer A. R., *Int. J. Insect Morphol. Embryol.*, **18** (1989) 145.
[10] Kirschner S., Kleineidam C. J., Zube C., Rybak J., Grünewald B. and Rössler W., *J. Comp. Neurol.*, **499** (2006) 933.
[11] Lieke E. E., *Eur. J. Neurosci.*, **5** (1993) 49.
[12] Galizia C. G., Sachse S., Rappert A. and Menzel R., *Nat. Neurosci.*, **2** (1999) 473.
[13] Gelperin A. and Flores J., *J. Neurosci. Methods*, **72** (1997) 97.
[14] Sachse S. and Galizia C. G., *J. Neurophysiol.*, **87** (2002) 1106.
[15] Galizia C. G., McIlwrath S. L. and Menzel R., *Cell Tissue Res.*, **295** (1999) 383.
[16] Hourcade B., Perisse E., Devaud J. M. and Sandoz J. C., *Learn. Mem.*, **16** (2009) 607.
[17] Galizia C. G. and Menzel R., *J. Insect Physiol.*, **47** (2001) 115.
[18] Haase A., Rigosi E., Trona F., Anfora G., Vallortigara G., Antolini R. and Vinegoni C., *Biomed. Opt. Express.*, **2** (2011) 131.
[19] Moreaux L. and Laurent G., *Front. Neural Circuits*, **1** (2007) 2.
[20] Müller D., Abel R., Brandt R., Zöckler M. and Menzel R., *J. Comp. Physiol. A*, **188** (2002) 359.
[21] Krofczik S., Menzel R. and Nawrot M. P., *Front. Comput. Neurosci.*, **2** (2008) 9.
[22] Yamagata N., Schmuker N., Szyszka P., Mizunami M. and Menzel R., *Front. Syst. Neurosci.*, **3** (2009) 16.
[23] Galizia C. G. and Vetter R., *Optical methods for analyzing odor-evoked activity in the insect brain*, in *Advances in Insect Sensory Neuroscience*, edited by Christensen T. A. (CRC press, Boca Raton) 2004, pp. 349-392.
[24] Peele P., Ditzen M., Menzel R. and Galizia C. G., *J. Comp. Physiol. A*, **192** (2006) 1083.
[25] Sachse S., Rappert A. and Galizia C. G., *Eur. J. Neurosci.*, **11** (1999) 3970.
[26] Laurent G., *Nat. Rev. Neurosci.*, **3** (2002) 884.
[27] Faber T. and Menzel R., *Naturwissenschaften*, **88** (2001) 472.